

## CHAPTER A-7 PROBABILISTIC LIMIT STATE ANALYSIS (RELIABILITY ANALYSIS)

### A-7.1 Key Concepts

The traditional factor-of-safety approach to limit state problems provides limited insight into failure probability. For example, typically, conservative input values (shear strength and water pressures) are assumed in stability analysis, and if the resulting factor of safety (FS) satisfies established criteria, the likelihood of failure is considered "low," but it is not quantified. The minimum FS required to produce a particular low value of probability depends on the material types and available data. A steep slope in dry granular material may have a very low probability of sliding with a factor of safety below 1.2; in that case, the main parameter of interest is the effective stress friction angle,  $\phi'$ , which varies over a fairly small range. If, instead, the slope is an excavation in saturated, soft clay, a much higher factor would be required to achieve the same probability, because undrained strength of clay has much greater variability and uncertainty than does the friction angle of sand. (How low of a probability is "low enough" to be acceptable depends on the situation, considering the consequences of failure and the cost of achieving a lower probability, as described elsewhere in this manual.)

Limit state analyses of concrete or embankment dams or levees are not always easy to decompose into a simple event tree for risk analysis, for example, if there are several independent variables that affect stability, such as strengths of the various materials involved and piezometric levels in different portions of a slope. One could, of course, discretize the range of possible strength values for each material and the ranges of possible piezometric levels into many small increments, and combine all of them in an event tree. However, with ten branches for five ranges of Material A strength, each leading to five branches for Material B strength, each leading to four branches for the piezometric level at Point 1, and so on, the number of branches and nodes would rapidly become intractable. A practical alternative is to develop probability distributions for the various parameters, and apply Monte Carlo (MC) analysis to determine the probability that the actual factor of safety is below some threshold value associated with



instability or other type of bad performance. That is the main subject of this chapter. Also covered is the First Order Second Moment (FOSM) method, a mathematically simpler, though somewhat less precise, approach to the same problem that can be performed using output from most analysis programs. Further discussions of MC and FOSM analyses and a general discussion of probabilistic analyses are included in Christian (2004).

Probabilistic limit state analysis is most likely to be applied to a possible future condition, such as unprecedented water levels against a levee, a proposed excavation, earthquake loading, or the effect of increased rainfall on an existing landslide. For those cases, it may not be possible to predict pore-water pressures or soil shear strengths with sufficient precision to analyze the slope deterministically and produce a single "correct" FS. For an existing structure with no anticipated change in loading, stability has been observed and pore pressures may be monitored, but one still might want to assess how close it is to the verge of instability in case of some unanticipated condition like plugging of drains.

The type of probabilistic stability analysis described in this chapter is sometimes referred to as "reliability analysis." When, for example, there are uncertainties about the shear strength and extent of liquefied foundation soils, reliability analysis can be useful for assessing the conditional probability of slope instability, given occurrence of an earthquake. Reliability analysis is typically not used on its own, as the sole method for estimating failure probability. Tempered by engineering judgment and full awareness of the biases and uncertainties that affect stability (or other) calculations, it is, however, a useful tool to inform expert judgment on conditional probabilities to be used in an event tree or other application.

For the purposes of this chapter, the probability of unsatisfactory performance is generally defined as the probability that the FS is less than 1.0. Other threshold values can be used. For example, if the dam or levee is particularly susceptible to deformation damage, a value of the safety factor slightly greater than 1.0 may better define the threshold for unsatisfactory performances (El-Ramly et al., 2002), and the probability of FS being below that value could be calculated instead.

In performing a probabilistic analysis, for example, to estimate the probability of sliding failure, either the factor of safety or the driving and resisting forces are characterized by probability distributions, rather than point values. The latter is illustrated in Figures A-7-1a and -1b. Each shows the Probability Distribution Functions (PDFs) for driving force and resisting force in blue and orange, respectively. The *mean* forces and the *mean* factor of safety are the same in both figures, but the driving and resisting forces are more precisely determined or constrained in A-7-1a. It can be seen that the chance that the driving force is greater than the resisting force is much greater in A-7-1b. (By numerical integration or Monte Carlo trials, one would find that the probabilities are about 0.001 for the well-constrained example, and 0.04 in the poorly constrained example.)

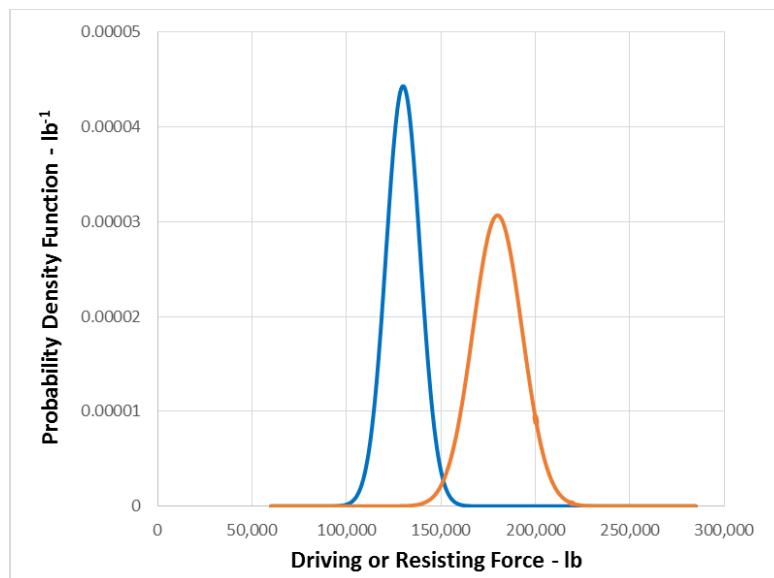


**Figure A-7-1a Probability Distribution Functions for Well-Constrained Driving and Resisting Forces**

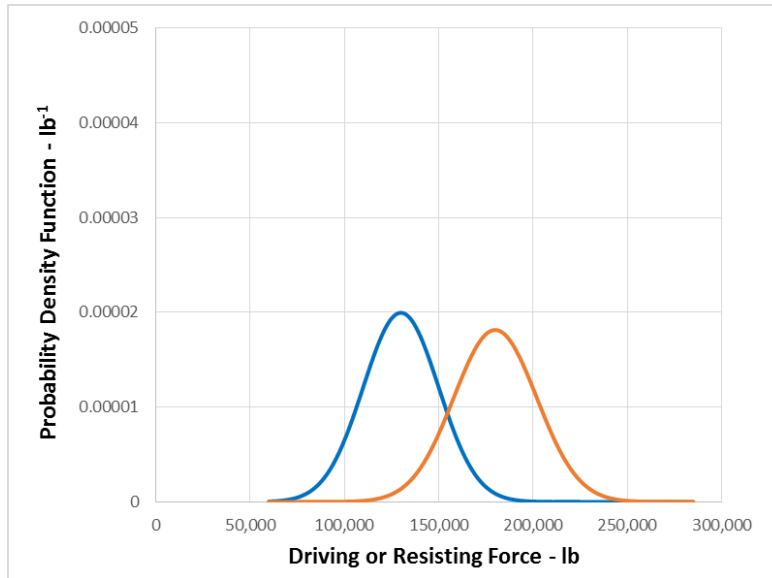


**Figure A-7-1b Probability Distribution Functions for Poorly Constrained Driving and Resisting Forces.**

With the availability of commercial computer analysis tools, MC reliability analysis has become much easier to perform. MC analysis using estimated PDFs for various input parameters (material shear strengths, uplift pressures, geometric conditions, etc.) is used most commonly to develop a PDF for the factor of safety. From that, the probability that the FS is less than 1.0 (or other value representing unsatisfactory performance) can be estimated. MC analysis is a built-in feature of some stability programs (e.g. GRAVDAM for concrete gravity dams and SLOPE/W for embankment dams). There are also macro add-ins that make it possible to perform the same functions using a spreadsheet program like Microsoft® Excel, provided a deterministic stability analysis can be programmed in the spreadsheet. Available add-ins include Palisade Corporation's Decision Tools Suite (which includes the @Risk module), ModelRisk by Vose Software, and Crystal Ball by Decisioneering, Inc. (Very simple MC analysis can also be done using the built-in features of Microsoft® Excel.)

The stability programs do have limitations, however. Not all of them have the ability to display sensitivity rank coefficients to describe the relative importance of variation in the different input parameters (described below); hence, some additional judgment and sensitivity runs of the MC model may be needed. Additionally, if none of the Monte-Carlo trials produce calculated factors

of safety less than 1.0, SLOPE/W indicates that the probability of failure is zero. The probability is not actually zero but is likely a small number out on the tail of the distribution. In addition, the MC analysis addresses only uncertainty in the stability input parameters, such as material properties and pore pressures, not uncertainty in the stability analysis procedure, or potential errors or misunderstanding. The risk analyst must apply judgment in evaluating the numerical results and estimating probabilities. When it calculates the reliability index (described below), SLOPE/W assumes that the factor of safety fits a normal distribution function, which is not necessarily so. GRAVDAM incorporates a cracked base analysis that must also be used with caution – refer to the chapter on Concrete Gravity Dams.

To use the Monte Carlo approach in a spreadsheet, the standard deterministic equations for calculating the factor of safety are programmed into a spreadsheet, but instead of the input parameters having single values, they are entered as random variables with assigned PDFs. Then, instead of calculating a single value for the factor of safety, the calculation is performed many (often thousands of) times, each time with parameter values sampled according to their respective PDFs, so that each trial produces a possible value of the FS. The probability of failure may be considered to be equal to the fraction of the trials that produced  $FS < 1.0$  (or other threshold value). Alternatively, a probability distribution function can be fitted to the safety factors resulting from the numerous Monte Carlo trials, with the probability of  $FS < 1.0$  being calculated from the form of the PDF. Example problems follow.

#### **A-7.2 Example: FOSM and MC Analysis for Heave at the Toe of a Levee**

The probabilistic approach can be applied to the assessment of safety against heave at the toe of a dam or levee, by any of several different methods that include Monte Carlo simulation and the First Order Second Moment (FOSM) method. This example will provide details of the FOSM method and a comparison of Monte Carlo and FOSM analyses. Further details of the FOSM method can be found in Wolff (1994) and USACE Engineer Technical Letter 1110-2-556.

Levees are often constructed in a geologic environment where a thin clay blanket exists over a thick pervious sand aquifer, and levee evaluations consider the potential for heave of this thin

clay blanket due to pore pressures in the pervious aquifer. This geometry is shown in Figure A-7-2.

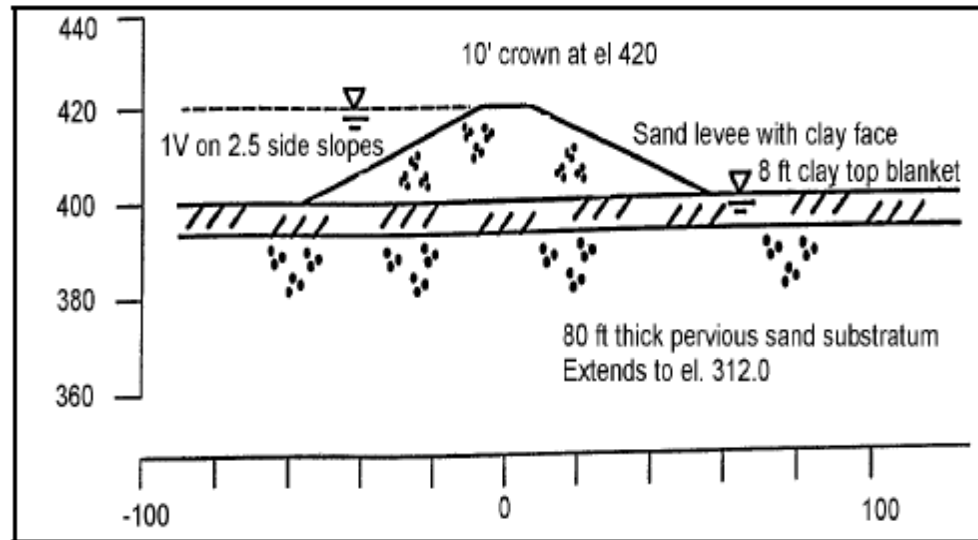


**Figure A-7-2 Model Geometry for Levee Heave Calculation**

The factor of safety against heave can be calculated by comparing the gradient across the clay blanket at the levee toe to the critical gradient for the clay blanket ( $FS = i_{crit}/i$ ). The gradient at the levee toe can be calculated by either developing a seepage analysis in a finite element method program such as SEEP/W or using Blanket Theory in closed form equations (TM 3-424). This example assumes an infinite length foundation with a semipervious clay blanket. The gradient across the clay blanket at the levee toe is calculated with the following equations from blanket theory. Figure A-7-3 illustrates the symbols used in the equations.



entrance and seepage exit are equal distances from the landside and waterside toes of the levee).

$H$  = Net head on the levee

$$x_3 = \sqrt{\frac{k_f z d}{k_b}}$$

**Equation A-7-3**

Where:

$k_b$  = Vertical hydraulic conductivity of the clay blanket

$k_f$  = Horizontal hydraulic conductivity of the pervious aquifer

$d$  = Thickness of the pervious aquifer

The critical gradient is calculated using the following equation:

$$i_{crit} = \frac{\gamma'}{\gamma_w}$$

**Equation A-7-4**

Where:

$\gamma'$  = Buoyant unit weight of clay blanket

$\gamma_w$  = Unit weight of water = 62.4 pcf

The total unit weight of the clay blanket was assumed to be 115 pcf (buoyant unit weight 52.6 pcf) giving a critical gradient of approximately 0.85 (assumed to be deterministic for this example). The pervious sand aquifer was assumed to have a horizontal hydraulic conductivity of  $1.0 \times 10^{-3}$  cm/sec.



For this evaluation of the probability of heave at the levee toe, the ratio of sand aquifer to clay blanket hydraulic conductivity, thickness of the clay blanket, and thickness of the sand aquifer were each varied by plus and minus one standard deviation, as shown in Table A-7-1.

**Table A-7-1 Variables in Levee Heave Analysis**

<b>Input Variable</b>	<b>Mean</b>	<b>Standard Deviation</b>
Ratio of aquifer horizontal hydraulic conductivity to blanket vertical hydraulic conductivity	1000	400
Thickness of clay blanket (ft)	8	2
Thickness of sand aquifer (ft)	80	5

The usual output of a FOSM analysis is the reliability index,  $\beta$ , which is then used to calculate the probability of  $FS < 1.0$ . To calculate  $\beta$ , the FOSM method, described below, uses a Taylor series expansion, simplified by using only the first term (hence, "First Order"). The expected value of the loading (in this case, the vertical gradient through the blanket layer at the levee toe) is calculated using the expected value of all random variables in the analysis, for comparison with the critical gradient assumed to cause heave (0.85 for this example problem). Each random variable is then varied by plus and minus one standard deviation (one at a time) to calculate the gradient with each change in the variable. The variance between the gradient calculated at plus and minus one standard deviation for each random variable is then calculated by taking the difference between the calculated gradient values. The total variance of the gradient is the sum of each of the variance calculations for each random variable. The expected value of the gradient calculated using the expected values for each random variable and the total variance are then used to calculate the reliability index and the probability of  $FS < 1.0$ .

The FOSM evaluation was performed for water levels on the floodside of the levee ranging from the levee toe (El 400 ft) to the levee crest (El 420 ft). The results of the calculation for the

probability of heave at the levee toe with water at the levee crest are shown in Table A-7-2, and the calculations included in this table are detailed below. The pink cells show the change in hydraulic conductivity ratio by plus and minus one standard deviation. These two rows show the calculation of the gradient with the change in hydraulic conductivity. The rows with the orange cells show the calculation of the gradient with the change in thickness of the blanket layer by plus and minus one standard deviation, and the rows with the green cells show the calculation of the gradient with the change in thickness of the pervious aquifer. The expected value of the gradient with the mean values of all the input parameters, E[i], is 1.170, as show in Table A-7-2.

**Table A-7-2 FOSM Calculations for Water Surface at Levee Crest**

WSE (ft) =		420		Head (ft) =		20									
Kf (cm/s)	Kb (cm/s)	kf/kb	z (ft)	d (ft)	x3 (ft)	s	ho	l	Variance Component	% of Variance					
1.00E-03	1.00E-06	1000.0	8	80	800	910	9.357	1.170							
1.00E-03	1.67E-06	600.0	8	80	620	730	9.185	1.148							
1.00E-03	7.14E-07	1400.0	8	80	947	1057	9.451	1.181	0.0003	0.3%					
1.00E-03	1.00E-06	1000.0	6.0	80	693	803	9.265	1.544							
1.00E-03	1.00E-06	1000.0	10.0	80	894	1004	9.421	0.942	0.0906	99.7%					
1.00E-03	1.00E-06	1000.0	8	75	775	885	9.337	1.167							
1.00E-03	1.00E-06	1000.0	8	85	825	935	9.375	1.172	0.0000	0.0%					
		K Ratio	blanket T	sand T					Total	0.0909		100%			
		Expected value		E[i] =		1.170		E[ln i] =		0.124					
				Var[i] =		0.091									
				Std. Dev. [i] =		0.301		sigma [ln i] =		0.254					
				COV[i] =		0.258									
				i critical =		0.850		ln(i critical) =		-0.163		Pr(f)=		87.11%	
				FS =		0.73						Beta=		-1.13	

A variance is calculated for each random variable, as shown in the last two columns of Table A-7-2. As shown in the equation below, the variance is the difference in the gradient when a random variable is varied by plus and minus one standard deviation. The variance component for each random variable is calculated using the following equation.

$$Var\ component = \left( \frac{\partial i}{\partial (k_f/k_b)} \right) \sigma_{k_f/k_b}^2 \approx \left( \frac{i_+ - i_-}{2\sigma_{k_f/k_b}} \right)^2 \sigma_{k_f/k_b}^2 = \left( \frac{i_+ - i_-}{2} \right)^2 \quad \text{Equation A-7-5}$$

Where:

$i_+$  = Gradient when random variable of interest is increased by  $1\sigma$

$i_-$  = Gradient when random variable of interest is decreased by  $1\sigma$

For Table A-7-2, the variance component for the blanket to aquifer hydraulic conductivity ratio is 0.0003. Total variance (Var) is the sum of the variance calculations for each random variable. As shown in Table A-7-2, it is 0.0909 for this calculation. The standard deviation of  $i$ , ( $\sigma_i$ ), is the square root of the variance, which is 0.301 for this calculation. The coefficient of variation of  $i$  is given by the following equation and is 0.258 for this calculation.

$$V_i = \frac{\sigma_i}{E[i]} \quad \text{Equation A-7-6}$$

The exit gradient is assumed to be a lognormally distributed random variable with probabilistic moments  $E[i] = 1.170$  (expected value of exit gradient) and  $\sigma_i = 0.301$ . If the gradient is lognormally distributed, then  $\ln(i)$  is normally distributed. The standard deviation of the natural log of  $i$  is

$$\sigma_{\ln i} = \sqrt{\ln(1 + V_i^2)} \quad \text{Equation A-7-7}$$

In this calculation,  $\sigma_{\ln i} = 0.254$ . The expected value of the natural log of  $i$  is calculated using the following equation.

$$E[\ln i] = \ln E[i] - \frac{\sigma_{\ln i}^2}{2} \quad \text{Equation A-7-8}$$

For this calculation  $E[\ln i] = 0.124$ . As calculated above, the critical gradient at this site is 0.85, and the probability of failure is assumed to be the probability that  $\ln(i)$  is greater than  $\ln(0.85)$  or in other words, the probability that the  $FS < 1.0$ . This probability can be evaluated two ways using normal distribution functions built into Excel. The first equation is:

$$\begin{aligned} Pr_f &= 1 - \text{norm.dist}(x, \text{mean}, \text{std.dev}, \text{cumulative}) \\ &= 1 - \text{norm.dist}(-0.163, 0.124, 0.254, \text{TRUE}) = 87.11\% \end{aligned}$$

where:

*norm.dist* = function to return the normal distribution for the specified mean and standard deviation

$$x = \ln i_{crit}$$

$$\text{mean} = E[\ln i]$$

$$\text{std.dev} = \sigma_{\ln i}$$

*cumulative* = TRUE to return the cumulative distribution function, FALSE to return the probability mass function

The second way of calculating the probability is to calculate the reliability index using the following equation:

$$\beta = \frac{\ln i_{crit} - E[\ln i]}{\sigma_{\ln i}} \quad \text{Equation A-7-9}$$

This equation yields a reliability index of -1.13. The probability of FS<1.0 is then calculated using the following equation in Excel:

$$Pr_f = 1 - \text{norm.s.dist}(z, \text{cumulative}) = 1 - \text{norm.s.dist}(-1.13, \text{TRUE}) = 87.11\%$$

where:

*norm.s.dist*= function to return the standard normal distribution (has a mean of zero and a standard deviation of one). This function replaces the use of a table of standard normal curve areas.

$z$  = reliability index,  $\beta$

*cumulative*= TRUE to return the cumulative distribution function, FALSE to return the probability mass function

For this analysis when the water elevation is at the levee crest, the probability of FS<1.0 is 87.11%, as shown in Table A-7-2. The probability of FS<1.0 can also be calculated for lower water elevations. The results of these calculations are plotted in Figure A-7-4.

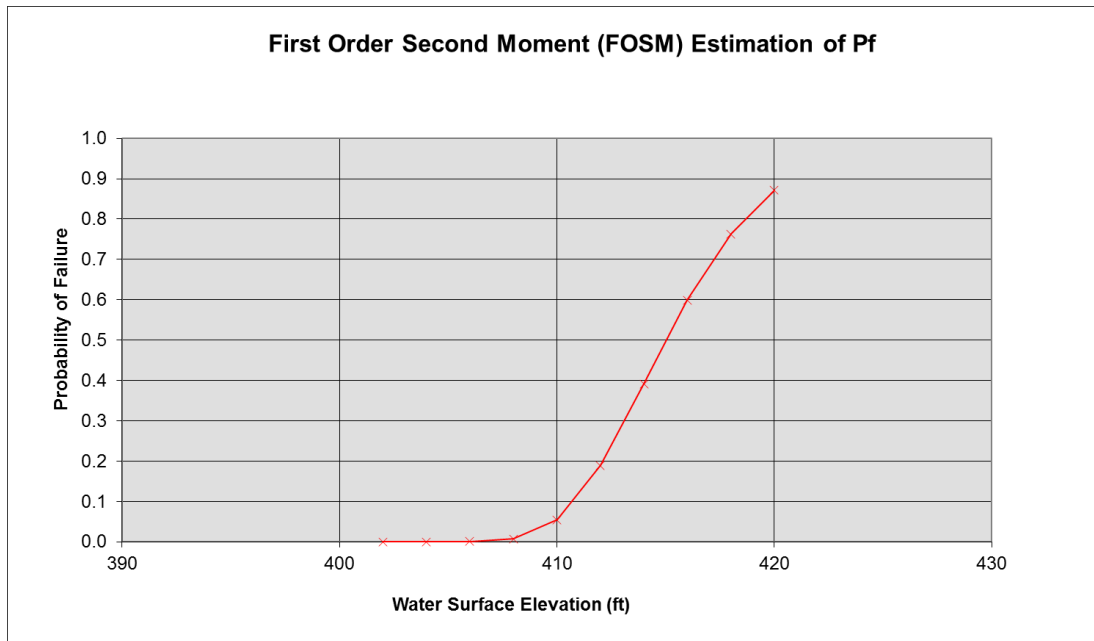


**Figure A-7-4 Probability of Levee Heave using FOSM Methods**

Reliability analysis such as FOSM is typically not used as the sole method for estimating failure probability, and the results of such analysis must be moderated using engineering judgment. In addition, the results may change depending on which variables are assumed to vary in the analysis. In the example above, the thickness of the blanket,  $z$ , provides the largest contribution to the variance as shown in Table A-7-2. If this variable is assumed to be constant in the analysis, the probability of  $FS < 1.0$  will change. If one of the other two variables, sand to blanket hydraulic conductivity or aquifer thickness, are assumed to be constant in the analysis, the probability of  $FS < 1.0$  is largely unchanged.

FOSM methods can also be used to calculate levee heave when a finite-element-method seepage analysis is performed and Monte Carlo simulations require too many iterations. For each change in material properties, a separate seepage analysis is performed. The excess pore pressure at the levee toe beneath the clay blanket is measured from each analysis and the gradient across the blanket is calculated. These gradients will then be used in the FOSM analysis to calculate the probability of heave as discussed above.

The heave analysis shown above can also be performed using a Monte Carlo simulation. A Monte Carlo simulation was performed using the software @Risk. The equations from blanket theory were programmed into an Excel spreadsheet. In this simulation, truncated normal distributions (truncated to 2 standard deviations above and below the mean value based on an understanding of the site characteristics) were input for the variables used to model the sand/blanket hydraulic conductivity ratio, the blanket thickness, and the sand thickness. These values are shown in Table A-7-3. Normal distributions are often truncated because the standard normal distribution is unbounded which can result in negative values that may not make sense. The @Risk function for the blanket thickness,  $z$ , for example, is:

RiskNormal(8,2,RiskTruncate(4,12)).

**Table A-7-3 Variable Distributions for Monte Carlo Simulation**

<b>Variable</b>	<b>Mean</b>	<b>Standard Deviation</b>	<b>Min</b>	<b>Max</b>
$k_f/k_b$	1000	400	200	800
$z$ (ft)	8	2	4	12
$d$ (ft)	80	5	70	90

After entering the input distributions in the spreadsheet cells, the factor of safety cell is selected as the output and the simulation settings are adjusted. In this case, 10,000 trials were specified. For each trial, each input parameter is sampled according to its probability density function, and an individual factor of safety is calculated. This results in a record of the calculated factors of safety for the entire simulation. It is a simple matter to sort the output factors of safety in ascending or descending order using the “sort” command of the spreadsheet program. The probability of  $FS < 1.0$  is taken as the number of trials with calculated factor of safety less than 1.0 divided by the total number of trials. In the case with the water surface at the levee crest, 9,590 trials produced a factor of safety less than 1.0. Therefore, the probability of  $FS < 1.0$  is estimated to be 9,590/10,000 or 0.959.

The results are shown in Table A-7-4 and compared to the FOSM results. This comparison indicates that FOSM evaluations and Monte Carlo simulations provide similar trends in results. However, the use of a different distribution, such as a triangular distribution or non-truncated normal distributions may provide different results so the distribution of any variable should be carefully considered. The first three Monte Carlo simulations (at water levels between 402 ft and 406 ft) did not give any factors of safety less than 1.0 indicating the probability of failure is less than 1/10,000. It should be noted that when the Monte-Carlo analysis did not return any factors of safety less than 1.0 in 10,000 iterations, the probability of failure was set to zero, although a reliability index could have been calculated and a probability based on the tails of a fitted distribution could have been estimated as described later. The FOSM results give similar results for water elevations 402 ft and 404 ft, but give a higher probability of heave at 406 ft.

**Table A-7-4 Comparison of Monte Carlo and FOSM Analysis Results**

<b>Water Level</b>	<b>Monte Carlo Simulation Probability of Heave at Levee Toe</b>	<b>FOSM Analysis Probability of Heave at Levee Toe</b>
402	0	0
404	0	9.24E-06
406	0	0.00015
408	0.0088	0.0066
410	0.079	0.055
412	0.22	0.19
414	0.43	0.39
416	0.66	0.60
418	0.85	0.76
420	0.96	0.87



To help understand which input parameter distributions have the greatest effect on the results, @Risk provides a list of correlation (Spearman Rank) coefficients. Those input distributions with the highest positive or negative correlation coefficients affect the results most. A positive coefficient means the variable is positively correlated with the results (as the variable increases the factor of safety also increases), and similarly a negative coefficient means the variable is negatively correlated with the results (when the variable increases, the factor of safety decreases). For example, an increase in pore pressure would result in a decrease in factor of safety, as would be expected.

For the example just described, the coefficients are shown in Table A-7-5. It can be seen that the thickness of the clay blanket,  $z$ , affects the results the most, which is consistent with what was observed in the FOSM analysis. The distributions that are input to the analysis, while accounting for uncertainty, in themselves are usually not well constrained. Therefore, an important use of this table is to identify which distributions should be considered for parametric or sensitivity evaluations. For example, in this case we may have had limited boring and mapping information to estimate the blanket thickness and wish to know how the probability of  $FS < 1.0$  would change if the mean blanket thickness was 9 feet with a standard deviation of 6 feet. In the MC analysis, the normal distribution of the blanket thickness was truncated at 0 feet and 21 feet. Running that analysis indicated the mean factor of safety for each water level increased, but for the water levels below 414, the probability of  $FS < 1.0$  also increased as shown in Table A-7-6 when compared to table A-7-4.

**Table A-7-5 Correlation coefficients for water surface at the levee crest**

<b>Rank</b>	<b>Name</b>	<b>Cell</b>	<b>Correlation</b>
<b>1</b>	$z$	\$B\$4	1.0
<b>2</b>	$k_f/k_b$	\$E\$4	-0.06
<b>3</b>	$d$	\$H\$4	0

**Table A-7-6 Comparison of Monte Carlo and FOSM Sensitivity Analysis Results**

<b>Water Level</b>	<b>Monte Carlo Simulation Probability of Heave at Levee Toe</b>	<b>FOSM Analysis Probability of Heave at Levee Toe</b>
402	0.027	0.0029
404	0.063	0.023
406	0.11	0.06
408	0.16	0.108
410	0.23	0.16
412	0.30	0.21
414	0.38	0.27
416	0.46	0.32
418	0.55	0.37
420	0.62	0.41

Apparently, at lower river stages, the probability of  $FS < 1$  comes only from the worst "perfect storm" combinations of parameters. If you increase the probability of the thinnest blankets by increasing the standard deviation a lot relative to the increase in the mean, you would increase the probability of "thin" blankets and  $FS < 1$ . The reverse would happen in the high-river cases, as observed because, by increasing both the mean and the standard deviation, the number of cases with greater thickness increased, reducing the number with  $FS < 1$ . As can be seen, a change in the input distribution for the key variables can have an effect (sometimes unpredictable upon initial blush) on the results, and sensitivity analyses can help to establish a range or distribution of probabilities for input to an event tree.

### A-7.3 Example: RCC Gravity Dam Stability

The probabilistic method is also applicable to sliding of concrete structures. For example, construction of a 160-foot-high roller-compacted concrete (RCC) gravity dam in a wide canyon was suspended for winter shut down after the RCC reached a height of 20 feet. The following construction season, the cold joint surface of the previous year was thoroughly cleaned and coated with mortar, and the remainder of the dam was placed. A gallery was constructed such that the gallery floor would be about 5 feet above tailwater during PMF conditions. A line of three-inch-diameter drains, spaced at 10 feet, was angled downstream from the gallery, intersecting the cold joint about 28 feet downstream of the axis. Although a 3.5-foot-high parapet wall was constructed on the upstream side of the dam crest, the spillway was sized to pass the probable maximum flood (PMF) without encroaching on the wall. Due to concerns about the strength of the cold joint, five six-inch diameter cores were taken one year later. Two of the five cores were not bonded at the lift joint. The remaining three were tested in direct shear at varying normal stresses. Although only three data points were generated, the results were well behaved as shown in Figure A-7-5. Accounting for about 40 percent de-bonded area of the joint, it was determined that the design intent was still met. Several years later, the PMF was revised and a new flood-frequency analysis was performed. Although the new PMF did not overtop the dam, it encroached about 2.3 feet onto the parapet wall, with no significant change in the tailwater elevation. Additional stability analyses were undertaken to evaluate the likelihood of failure under the new loading condition.

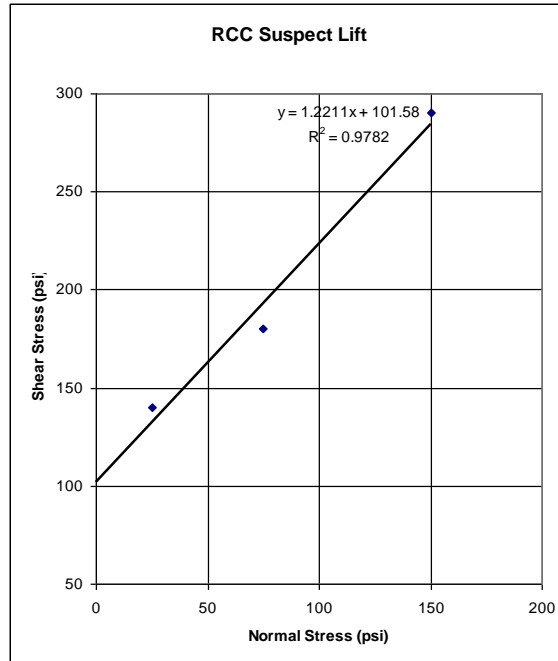


**Figure A-7-5 Direct Shear Test Results for Suspect RCC Lift Joint**

The dam cross section shown in Figure A-7-6 was used in the analysis. The vertical stress at the upstream face is calculated considering the standard beam-column equation from mechanics of materials:  $\sigma_v = P/A \pm Mc/I$  to account for the vertical load (P) and the moment (M) induced by the reservoir for the combined stress condition, as indicated by Watermeyer (2006). Initially, uplift along the cold joint is approximated by a bi-linear distribution of pressures, varying from full reservoir pressure at the upstream face, to a reduced pressure at the line of drains, to tailwater at the downstream face. The total head at the line of drains is approximated as  $F_d * (\text{Reservoir El.} - \text{Tailwater El.}) + \text{Tailwater El.}$ , where  $F_d$  is the drain factor (1-efficiency). The pressure head is determined by subtracting the elevation of the potential sliding surface from the total head, and the pressure head is converted to an uplift pressure for analysis. The effective stress is calculated along the potential sliding plane by subtracting the uplift pressure from the total stress, and where the effective stress is calculated to be tensile, no resistance is included for that portion of the plane. Since the locations of potential joint de-bonding are unknown, the cold joint was also assumed to be cracked to the point of zero effective stress in this case. Full reservoir pressure was assumed in the crack until it reached the drains. Then, approximate equations were used to adjust the drain factor to account for the crack length (Amadei et al.,

1991). These equations require the “allow circular reference” feature of Excel to iterate on a crack length. The factor of safety was then calculated from the familiar equation  $FS = [c'A + (W-U)\tan\phi']/D$ , where  $W$  is the vertical load,  $A$  is the bonded area,  $U$  is the uplift force, and  $D$  is the driving force taking into account both the downstream-directed reservoir load and the upstream-directed tailwater load.

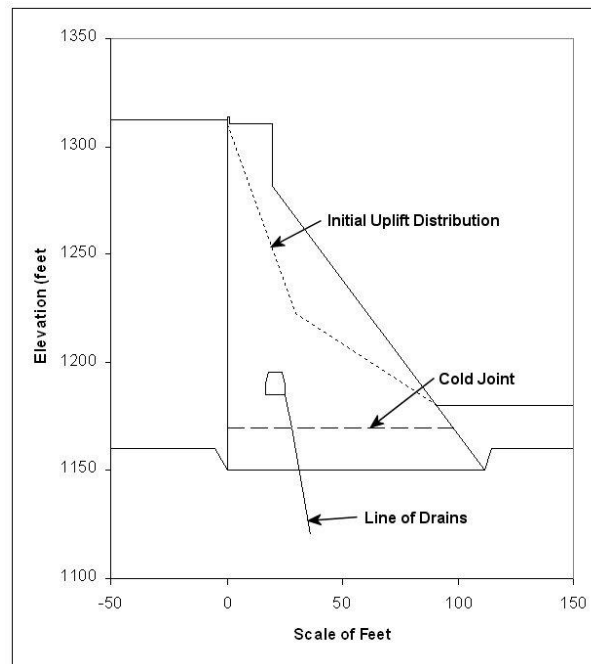


**Figure A-7-6 Cross-sectional Geometry of an RCC Gravity Dam**

The equations for limit equilibrium analysis were programmed into a spreadsheet. Input variables that were defined as distributions included the following: (1) drain factor  $F_d$ , (2) tangent of the intact friction angle on the potentially weak lift joint  $\phi'$ , (3) intact cohesion on the potentially weak lift joint  $c'$ , (4) percentage of the joint that is intact, and (5) the RCC unit weight. Table A-7-7 defines the distributions that were used.

**Table A-7-7 Summary of Concrete Input Properties**

<b>Property</b>	<b>Distribution</b>	<b>Minimum</b>	<b>Mode</b>	<b>Maximum</b>
Initial Drain Factor, $F_d$	Uniform	0.33	n/a	0.75
$\phi'$ (degrees)	Triangular	43	50	57
Intact $c'$ (lb/in <sup>2</sup> )	Triangular	50	100	150
Percent Intact	Triangular	43	60	71
Unit Weight (lb/ft <sup>3</sup> )	Uniform	146	n/a	152

The RCC unit weight, based on measurements from the core samples, had only limited variability, and a uniform distribution between the minimum and maximum measured values was used. For the other parameters:

- The initial drain factor was taken to be a uniform distribution based on piezometer measurements and experience with other concrete dams of similar geometry.
- The coring would suggest that about 60 percent of the lift surface was bonded, assuming the cores were not mechanically broken at that elevation during drilling. To estimate a likely range, the percentage was adjusted by assuming the drilling of two more holes yielded bonded lifts (upper bound estimate), or yielded unbonded lifts (lower bound estimate).
- Both the cohesion and tangent friction angle were defined as triangular distributions, with the peak or mode of the distribution estimated using the straight line fit shown in Figure A-7-5. High and low values were estimated based on experience with other direct shear tests on concrete joints, and interpolating other reasonable lines through the data points.

The minimum safety factor calculated from 10,000 iterations was 1.43, with a mean value of 2.42. The results are shown as a bar chart, with a normal distribution fitted to them in Figure A-7-7. The sensitivity analysis indicated the cohesion had the largest effect on the results, as shown in Table A-7-8, and additional sensitivity studies on that parameter would be appropriate.

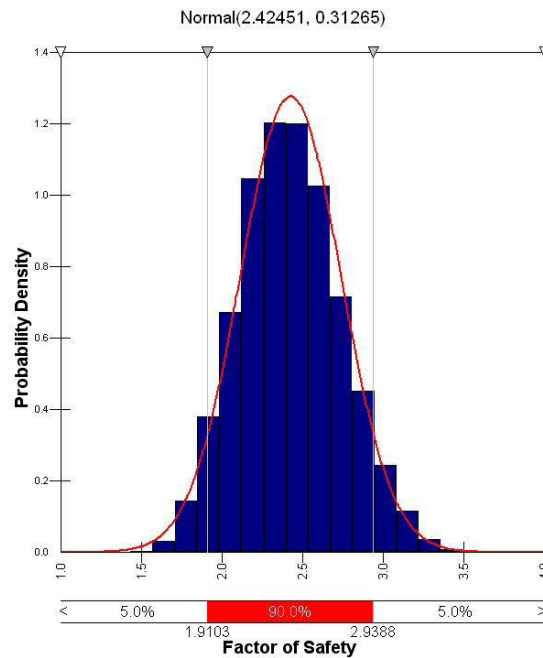


**Figure A-7-7 Output Factor of Safety Distribution for RCC Dam with a Fitted Normal Distribution Superimposed, Assuming Independence of Cohesion and Friction Angle.**

**Table A-7-8 RCC Dam Sensitivity Rankings**

Rank	Name	Cell	Regression
1	Intact Cohesion (psi)	\$B\$17	0.759
2	Tan(Friction Angle)	\$B\$16	0.412
3	Percent Intact	\$B\$18	0.369
4	Drain Factor	\$B\$15	-0.312
5	Concrete Density (pcf)	\$B\$19	0.097

Experience suggests that the cohesion and friction angle are negatively correlated. That is, as the friction angle becomes greater, a line that passes through the data would intercept the vertical axis at a lower cohesion value, and vice versa. @Risk allows the user to correlate input variables, such that in this case, a high value of cohesion will only be sampled with a low value of friction angle, and vice versa. Since there were limited data points upon which to base a correlation in this example, a negative correlation coefficient of 0.8 was selected, meaning that the highest cohesion value doesn't have to be associated with the absolute lowest friction angle, but the general trend of the correlation is maintained. The minimum factor of safety calculated with this correlation is 1.79, higher than if the correlation is not maintained, indicating that ignoring the correlation would be conservative in this case.

Since the factor of safety never dropped below 1.0 in any of the Monte Carlo trials, it is not possible to determine the probability of  $FS < 1.0$  directly as in the embankment dam example below. It is possible that increasing the number of trials would achieve better coverage of all possible permutations of the random variables and find some combinations that give  $FS < 1.0$ , which is an easy thing to test. In this case, however, with the most conservative assumptions allowed by the PDFs on input parameters, the stability analysis would not yield  $FS < 1.0$ ; instability is simply not possible within the assumptions of the analysis and its input parameters. It can really only be said that the probability of  $FS < 1.0$  is "small," but it is not zero because of potential errors or biases in the analysis or its inputs, that is, because of epistemic (model) uncertainty.

Although numerical estimates may not be very meaningful if the epistemic (model) uncertainty is not accounted for, this problem has sometimes been addressed by fitting a probability distribution to the FS results, and applying reliability theory. To do this, the "reliability index,"  $\beta$ , is introduced. It is simply the number of standard deviation units between the mean value and the value representing failure. Figure A-7-7 above shows the output factor of safety distribution for the first case (i.e., with cohesion and friction angle assumed to be independent of each other). Goodness-of-fit tests indicate the FS distribution follows a normal distribution quite well within the range of sampled output values. The reliability index, in this case relative to a safety factor of 1.0, is  $(FSAVG - 1.0)/\sigma_F$ , where  $FSAVG$  is the mean safety factor and  $\sigma_F$  is the standard



deviation of the safety factor distribution, or  $\beta = (2.425 - 1.0)/0.3126 = 4.56$ . There is a standard function in Microsoft Excel that allows one to estimate the probability of  $FS < 1.0$  directly from the reliability index, namely  $1 - \text{NORM.S.DIST}(\beta)$ . This gives the probability of  $FS < 1.0$  as  $2.6 \times 10^{-6}$ . This is a very low number, which should be expected, given the high mean factor of safety and the fact that the minimum value calculated in 10,000 iterations never dropped below 1.4. When the probability of failure is determined to be so far out on the tails of a distribution as in this case, the number generated in this fashion is highly uncertain and it is sensitive to the form assumed for the PDF. It may not be appropriate to report a quantitative probability produced this way, although the exercise to generate it can still be useful for understanding the problem, and reporting it with proper caveats can still be informative.

In some cases, the output factors of safety may not follow a normal distribution, but rather a lognormal distribution. For those situations, the same method can be used to estimate the probability of  $FS < 1.0$ . The only difference is that the reliability index is calculated with a different formula (Scott et al., 2001), as follows:

$$\beta_{\lognormal} = \frac{\ln\left(\frac{FS_{mean}}{\sqrt{1 + V_{FS}^2}}\right)}{\sqrt{\ln(1 + V_{FS}^2)}} \quad \text{Equation A-7-10}$$

Where  $FS_{mean}$  is the average factor of safety of the Monte Carlo output distribution and  $V_{FS}$  is the coefficient of variation for the factor of safety, equal to the standard deviation divided by the mean.

#### **A-7.4 Example: Screening-Level Check of Embankment Post-Liquefaction Stability**

Consider the homogeneous embankment dam shown in Figure A-7-8. The dam is in a seismically active area. What appears to be a continuous clean sand layer, approximately four to six feet thick, was encountered in three borings, approximately eight feet below the dam-foundation contact. The minimum corrected (N1)<sub>60</sub> blow count values encountered in this layer

varied from 13 to 15 depending on the boring. The toe of the dam is wet, indicating a high phreatic surface and saturated foundation materials in that area. Given that the sand layer liquefies, what is the probability of post-liquefaction instability as defined by  $FS < 1.0$ ?

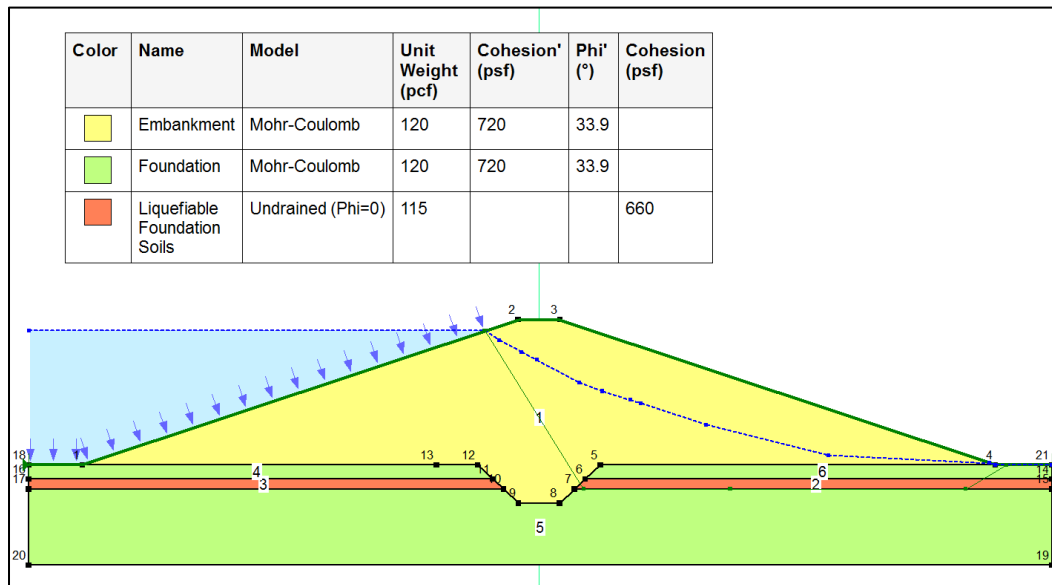


**Figure A-7-8 Example Embankment Dam Geometry**

It is necessary to perform rigorous stability analysis to identify the critical failure surface as well as the factors of safety for surfaces that may be of interest in terms of risk. The geometry shown in Figure A-7-8 was analyzed using SLOPE/W (Spencer Method). A surface passing through the liquefied layer and intersecting the upstream face below the reservoir surface at normal pool was one case that, if sliding occurred, would cause widespread damage, and therefore was evaluated here.

Input variables defined as distributions include: (1) effective stress cohesion of the embankment material ( $c'$ ), (2) effective stress friction angle of the embankment material ( $\phi'$ ), and (3) undrained residual shear strength of the liquefied sand layer ( $S_u$ ). No test results were available for the embankment materials. Therefore, the mean, standard deviation, maximum, and minimum values listed in Design of Small Dams (BOR, 1987) for SC material (see Table A-7-9) were used to define truncated normal distributions for simplicity and illustration purposes.

It should be noted that the strength values from Design of Small Dams likely came from tests on compacted construction samples and may not be totally representative of saturated embankment conditions. However, both  $c'$  and  $\phi'$  from Design of Small Dams are used in this example for illustration purposes, and have been negatively correlated in SLOPE/W meaning that higher friction angles are correlated with lower cohesion values and vice versa. The potential for correlation of the cohesion and friction angle is based on testing of numerous samples, and is discussed in one case as part of the previous example. The correlation was assumed to be -0.7 based on experience with similar materials. A correlation value can range from 0 to 1.0 (or -1.0) with 0 indicating no correlation and 1.0 (or -1.0) indicating that higher friction angles will always be correlated with higher (or lower) cohesion values.

**Table A-7-9 Summary of embankment input properties (SC)**

<b>Property</b>	<b>Minimum</b>	<b>Maximum</b>	<b>Mean</b>	<b>Standard Deviation</b>
Cohesion, $c'$ (lb/ft <sup>2</sup> )	101	1224	720	360
Friction Angle, $\phi'$ (degrees)	28.4	38.3	33.9	2.9

From the available information at the site, the non-liquefiable alluvial foundation soil was assumed to have similar material properties as the embankment soils. In addition, the unit weight of the embankment and foundation were assumed to be 120 lb/ft<sup>3</sup>. It is also assumed that the effective stress parameters listed in Table A-7-9 and unit weight are equally applicable above and below the phreatic surface.

Finally, the undrained residual shear strength of the liquefied foundation sand was estimated using curves developed by Seed and Harder (Seed et al., 2003). Upper and lower bound curves are provided as a function of corrected SPT blow count. It was assumed that a strength midway between the curves represented the best-estimate value (mode). A triangular distribution between the upper (920 lb/ft<sup>2</sup>) and lower (400 lb/ft<sup>2</sup>) bound values, with the mode at the best

estimate (660 lb/ft<sup>2</sup>), for an N1,60,cs of 14, was assigned to this input parameter. (It is recognized that more recent guidance on the selection of residual strengths exists, but for simplicity and illustration purposes the Seed and Harder relationship is used for this the example.) The unit weight of this layer was assumed to be 115 lb/ft<sup>3</sup>.

For this case, 10,000 trials were specified. For each trial, each input parameter is sampled according to its probability density function, and an individual factor of safety is calculated. SLOPE/W reports this as a probability of failure where failure is defined as a factor of safety less than 1.0. For this analysis, the deterministic factor of safety of 1.08 is shown in Figure A-7-9 and the probability of failure is approximately 24% as shown in Figure A-7-10.

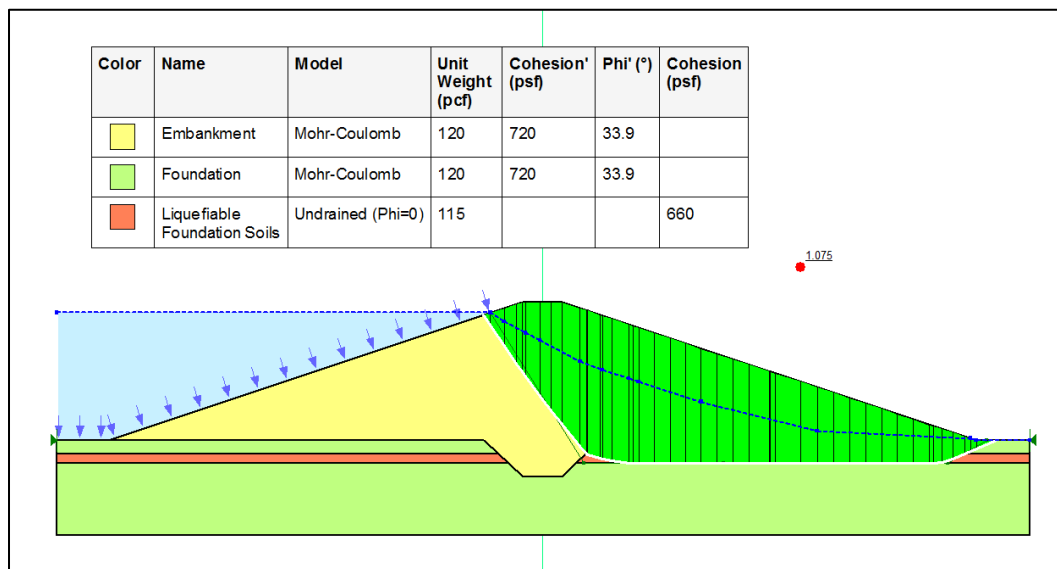


**Figure A-7-9 Results of Embankment Dam Analysis**

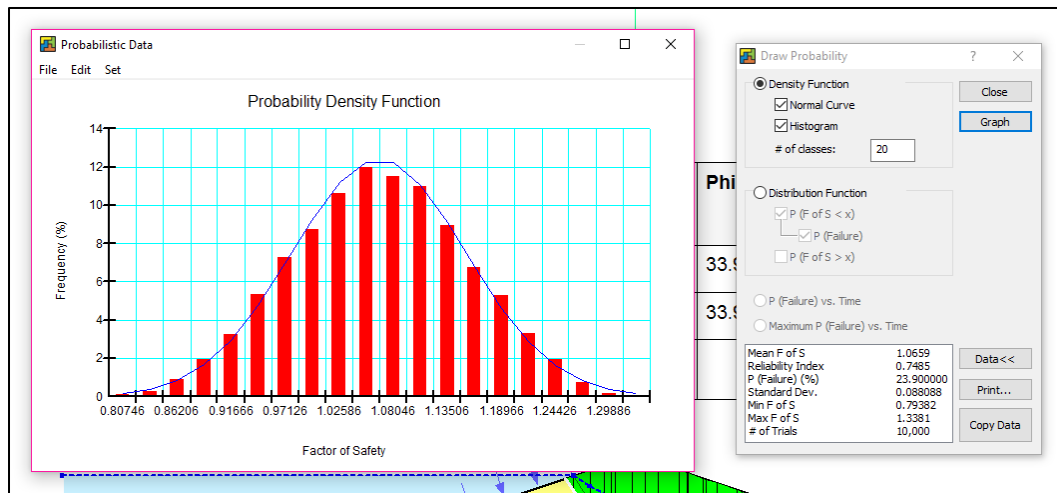


**Figure A-7-10 Results of Probabilistic Analysis in SLOPE/W**

It should be noted that  $FS > 1.0$  means the slope would be stable, but does not rule out dam failure by another potential failure mode; even if the embankment remains stable, deformation could result in transverse cracks through which erosion could occur. This must be considered in evaluating the overall risks posed by the dam and reservoir. In addition, surfaces with “entry” points further downstream should also be investigated to check for the potential for retrogressive sliding to cut the slope under the reservoir, following movement of the first slide.

If the probability of the factor of safety being less than a number other than 1.0 needs to be evaluated, SLOPE/W also provides a cumulative probability distribution function. As shown in Figure A-7-11, the probability of the factor of safety being less than 1.1 is approximately 64%.

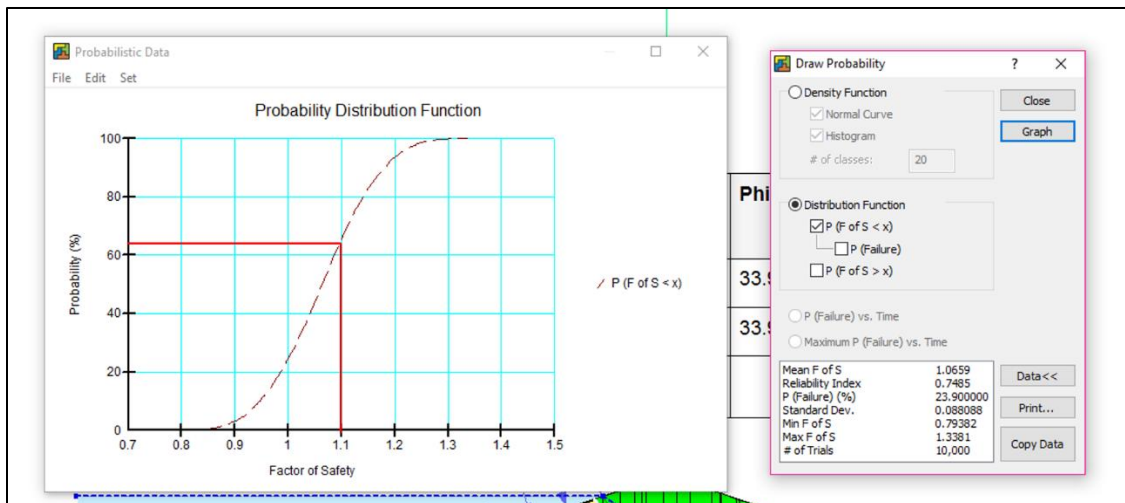


**Figure A-7-11 Probability Distribution Function in SLOPE/W**

#### A-7.5 Example: Foundation Rock Wedge Stability

During a corrective action study, it was verified that a concrete arch dam constructed in the 1920s was founded on a geometrically significant rock wedge. Due to concerns about the potential for static and seismic instability of the wedge, the dam was modified with the installation of a drainage adit in the right abutment. As indicated by the volume of the measured drain flows and by piezometer readings taken before and after the modification, the drainage tunnel was successful in lowering uplift pressures in the right abutment area. However, a subsequent jump in the piezometer readings (with no accompanying decrease in the drainage flows) led to renewed concern and further analysis. Three possible piezometric profiles were developed, and stability under both static and seismic conditions was re-evaluated using the finite-element method. The finite-element model of the dam/foundation system showed some limited movement occurring under strong seismic shaking and no movement under static conditions, even with the worst-case uplift scenario assumed. This information was used to develop the potential failure modes (PFM).

The static version of the right abutment foundation instability PFM included the following five events:

1. Reservoir surface exceeds the critical elevation
2. Base, side, and release planes exist in situ and are continuous
3. Critical wedge movement initiates
4. Movement is significant enough to cause concrete cracking
5. Arch forces cannot be redistributed and a breach occurs

Given the initiation of foundation wedge movement, the risk analysis team believed that the results of the seismic analysis could be used to inform the probabilities of events 4 (Movement is significant enough to cause concrete cracking) and 5 (Arch forces cannot be redistributed and a breach occurs). However, since no movement was predicted by the static finite element analysis results, the team struggled with how to estimate the probability of the initial foundation wedge movement absent seismic loading. Conceptually, the initiation of movement could be tied to a drop below 1.0 in the static safety factor, but the static safety factors calculated in previous limit equilibrium analyses were all significantly greater than 1.0. Given the relatively high static safety factors, the team was also not comfortable with the approach of using the neutral estimate (0.5) as a starting point and adjusting up or down based on the more/less likely factors. It was thought that such an approach could result in an unrealistically high probability estimate for this key event of the static PFM.

The decision was made to use a probabilistic limit state approach to help inform the probability estimates for foundation wedge movement initiation. The three-dimensional wedge stability solution of Pierre Londe (see Hendron, Cording, and Aiyer 1980) was programmed into a spreadsheet that included the following inputs for each joint plane, in addition to the weight and external force resultant: dip and dip direction; position of the wedge with respect to the joint plane (above or below it); the magnitude of the uplift force, and; the effective friction angle. For each set of inputs, the spreadsheet calculates the sliding mode and the sliding factor of safety (Figure A-7-12). As a check, the basic results of the spreadsheet, for each of the three foundation uplift scenarios, were compared to the results of the existing limit equilibrium analyses.

Next, the deterministic inputs were changed to distributions, whose bounds were selected in accordance with the uncertainty considered to apply to the parameters. For example, the dip and dip direction of each of the defining discontinuities was expanded to the original value  $\pm 3^\circ$ . The base and side plane friction angles were entered as triangular distributions bounded by  $39^\circ$  and  $48^\circ$  (mode  $45^\circ$ ) and by  $39^\circ$  and  $52^\circ$  (mode  $50^\circ$ ), respectively. Finally, the upper and lower bounds of the resultant force magnitude for each uplift scenario were defined by varying the original magnitude by  $\pm 20$  percent. The rationale for each of the uncertainty ranges selected was discussed by the team and would be documented in the risk report. A Monte Carlo simulation consisting of 100,000 trials was then performed for each of the three foundation uplift scenarios, with the Factor of Safety (FS) defined as the simulation output.

For the “worst case” uplift scenario (static FS = 1.49), 55 of the 100,000 trials resulted in safety factors lower than unity. For the “best estimate” scenario (static FS = 1.59), 2 of the 100,000 trials resulted in safety factors lower than unity. For the “best case” scenario (static FS = 2.75), none of the trials resulted in safety factors lower than unity. Interpreting as probabilities, these results suggested wedge movement initiation probabilities of  $6 \times 10^{-4}$ ,  $2 \times 10^{-5}$ , and 0 for the “worst case”, “best estimate”, and “best case” foundation uplift scenarios, respectively. Note that these numbers are small enough to be outside the probability range over which most estimators are calibrated (see chapter on Subjective Probability and Expert Elicitation). They should therefore be interpreted as simulated frequencies (analogous to, but characterized by significantly more uncertainty than, the empirically derived internal erosion initiation probability base rates), rather than as subjective probabilities, when used as the starting point for estimation.

In addition to illustrating the application of the Monte Carlo method in developing probabilities to populate an event tree, this example is also relevant to the topic of expert elicitation. For computation of the conditional probability of sliding initiation, the team originally intended to use the above results to define a triangular probability distribution, but did not feel comfortable using a lower bound of 0, because of epistemic (model) uncertainty that may not have been fully accounted for. After considering the use of broader ranges for the inputs (rejected because it was



not considered defensible) and the use of a fitted output distribution (rejected because the results would be very sensitive to how the distribution was actually fitted), the team judged that  $1 \times 10^{-7}$  would be a reasonable lower bound, recognizing the potential, albeit small, for errors or biases in the stability model to result in stability being predicted when it would not actually occur.

Input the dip of joint set A (degrees)	13
Input the dip of joint set B (degrees)	43
Input the dip of joint set C (degrees)	65
Input the joint set A dip direction (CW w/r N)	116
Input the joint set B dip direction (CW w/r N)	115
Input the joint set C dip direction (CW w/r N)	6
Block is above (0) or below (1) Joint Set A?	0
Block is above (0) or below (1) Joint Set B?	0
Block is above (0) or below (1) Joint Set C?	1
Enter the estimated weight of the wedge	2.64E+08
Enter the magnitude of the water force along A	1.30E+07
Enter the magnitude of the water force along B	3.61E+07
Enter the magnitude of the water force along C	5.65E+07
Enter the x (E) component of Q	-1.63E+08
Enter the y (N) component of Q	-4.31E+07
Enter the z (UP) component of Q	3.56E+07
Enter $\phi_A$ , the Joint Set A friction angle	45
Enter $\phi_B$ , the Joint Set B friction angle	50
Enter $\phi_C$ , the Joint Set C friction angle	50
*****RESULTS*****	
The failure mode (see below) is failure mode #	5
The sliding factor of safety for the failure mode:	1.59085624
<b>List of possible failure modes:</b>	
1. The wedge will be unstable in the absense of cohesion	
2. The resultant force points into the rock	
3. The failure mode is sliding along $I_{BC}$	
4. The failure mode is sliding along $I_{AC}$	
5. The failure mode is sliding along $I_{AB}$	
6. The failure mode is sliding along plane A	
7. The failure mode is sliding along plane B	
8. The failure mode is sliding along plane C	

**Figure A-7-12 Input and Output Cells of the Spreadsheet used to Calculate the Stability of the Three-Dimensional Wedge**

The team felt that values at the lower end of the range were more likely to be “correct” than those at the upper end of the range, and initially adopted the triangular distribution shown in Figure A-7-13, with a lower bound and mode of  $1 \times 10^{-7}$  and an upper bound of  $6 \times 10^{-4}$ . It was subsequently recognized that the shape of this PDF did not capture the team's belief about the

lower end being more likely, and that its mean,  $2 \times 10^{-4}$ , was much higher than the team's "best estimate". After recognizing that they were accustomed to thinking in terms of a log scale, the team members realized that what had really been intended was something more like the distribution shown in Figure A 7 14, which is still triangular, but with a logarithmic horizontal axis. It has the same upper and lower bounds, but the mean is much smaller at  $1.9 \times 10^{-6}$ , more in keeping with the team's degree of belief. For computation in @Risk, this "log-triangular" distribution was approximated using the truncated log-normal distribution in Figure A 7 15, which has the same mean and bounds as the team's intended result. Note that the probability estimate selected for this event spans an uncertainty range of over three orders of magnitude. For this particular application, the team considered such a wide range to be appropriate, but concluded that the uncertainty could potentially be reduced through additional field data collection (e.g. the installation of additional piezometers), laboratory testing (direct shear), and modeling (updated, coupled, finite element analysis).

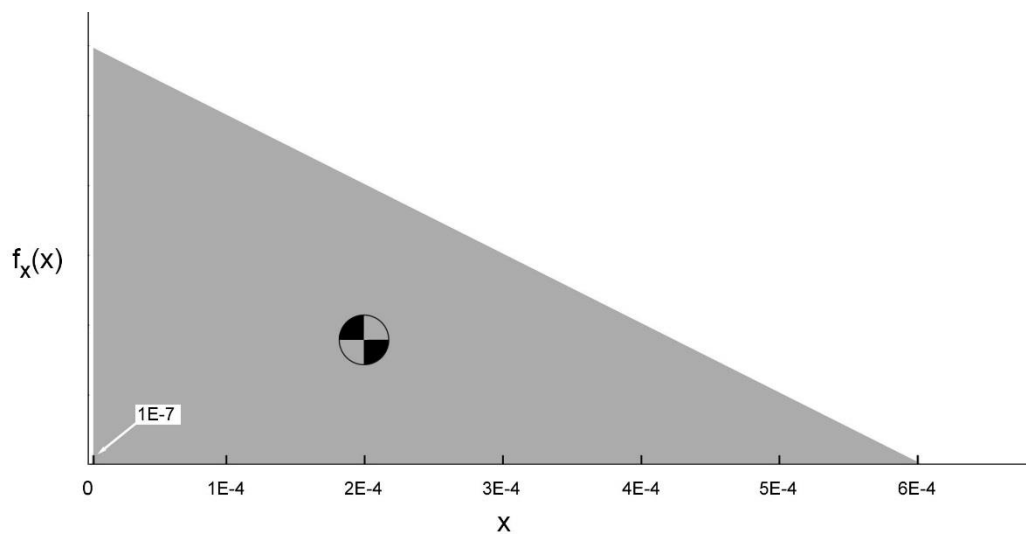


**Figure A-7-13 Triangular Probability Distribution Initially Selected by the Team for Foundation Wedge Movement Initiation**

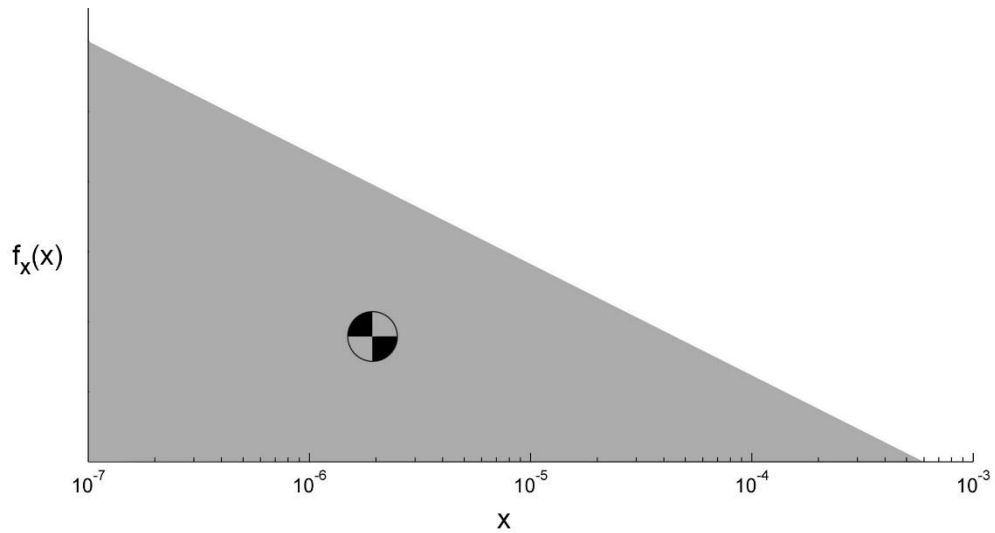


**Figure A-7-14 Log-Triangular Probability Distribution Actually Intended by the Team for Foundation Wedge Movement Initiation**

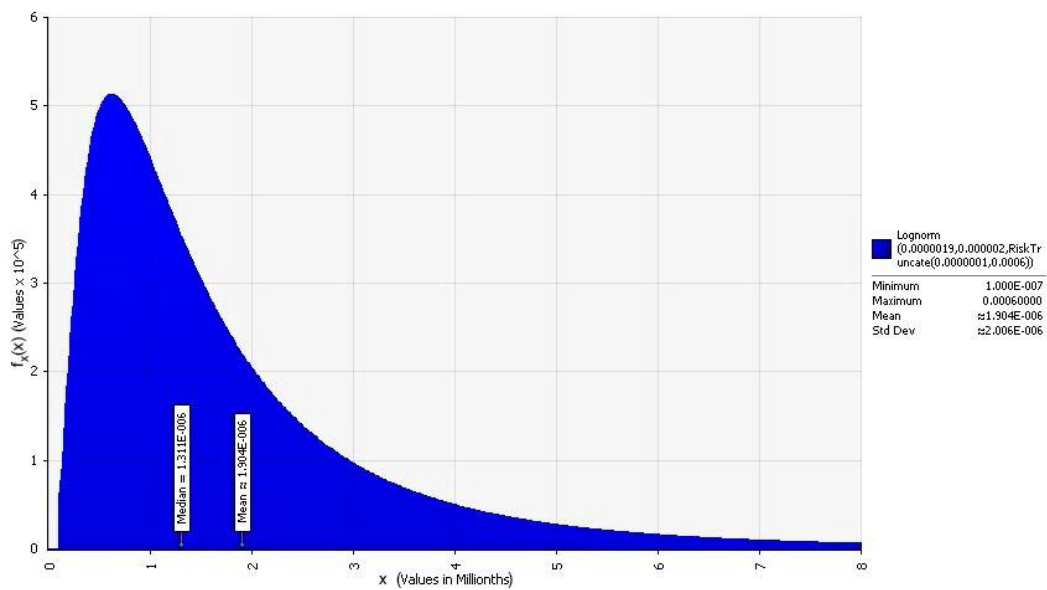


**Figure A-7-15 Truncated Lognormal Probability Distribution Ultimately Selected by the Team for Foundation Wedge Movement Initiation**

## A-7.6 Model Uncertainty

The preceding discussion provides methods for calculating probabilities considering uncertainties in the input parameters of engineering analyses, such as slope stability or heave analyses. This type of uncertainty is sometimes referred to as aleatory or parameter uncertainty. However, significant uncertainty also exists regarding how well the models used in the calculations actually reflect the real situation. This is sometimes referred to as epistemic or model uncertainty. Models are just that, limited approximations. Vick (2002) provides additional discussion concerning the limitations of models.

Some of the models used in the spreadsheet calculations previously described are simplifications of complex three-dimensional problems. For example, the equations used in the RCC dam example do not take into account shear resistance along the sides of the sliding block, and it would be much more difficult to account for that in the simple spreadsheet model. This creates a *conservative* bias in the FS calculations, and it is appropriate to interpret the results of the numerical reliability analysis in light of that. This could be done either within the reliability analysis, by adjusting the threshold FS that defines failure, or in the application, by adjusting the failure probability indicated by the reliability analysis before it is used in the event tree. Either way, the adjustment would include some element of subjectivity, and it has to be recognized that the adjustment is itself uncertain. (See the chapter on Subjective Probability and Expert Elicitation.)

Similarly, there may be simplifications in the model that create *unconservative* bias. For example, limit-equilibrium stability analysis does not account for strain incompatibility, the potential for one material in the sliding surface to be sheared past failure before the strength of another material is fully mobilized. It may be possible to address the bias by the same means as in the case of a conservative bias (i.e. by making adjustments at the subjective probability estimate level), provided there is adequate treatment of the uncertainty in any adjustments made.

## A-7.7 References

Amadei, B., T. Illangasekare, C. Chinnaswamy, D.I. Morris, "Estimating Uplift in Cracks in Concrete Dams," Proceedings, International Conference on Hydropower, Denver, Colorado, July 24-26, 1991.

Bureau of Reclamation, *Design of Small Dams*, Third Edition, Denver, CO, 1987.

Christian, J.T., "Geotechnical Engineering Reliability: How Well do We Know What We Are Doing," *Journal of Geotechnical and Geoenvironmental Engineering*, Volume 130, No.10, pp. 985-1003, 2004.

El-Ramly, H., N.R. Morgenstern, and D.M. Cruden, "Probabilistic Slope Stability Analysis for Practice," *Canadian Geotechnical Journal*, NRC Canada, Volume 39, pp. 665-683, 2002.

Hendron, AJ, Cording, EJ, and Aiyer AK. Analytical and Graphical Methods for the Analysis of Slopes in Rock Masses. Technical Report GL-80-2. U.S. Army Engineer Waterways Experiment Station, Vicksburg, MS. March 1980.

Olson, S. M. & Stark, T. D, "Liquefied strength ratio from liquefaction case histories," *Canadian Geotechnical Journal*, Volume 39, No. 3, pp 629–647, March, 2002.

Seed, R.B., K.O. Cetin, R.E.S. Moss, A.M. Kammerer, J. Wu, J.M. Pestana, M.F. Riemer, R.B. Sancio, J.D. Bray, R.E. Kayen, and A. Faris, "Recent Advances in Soil Liquefaction Engineering: A Unified and Consistent Framework," 26<sup>th</sup> Annual ASCE Los Angeles Geotechnical Spring Seminar, Long Beach, CA, April 30, 2003.

Scott, C.R., *Soil Mechanics and Foundations*, Applied Science Publishers, Ltd., London, Second Edition, 1974.

Scott, G.A., J.T. Kottenstette, and J.F. Steighner, “Design and Analysis of Foundation Modifications for a Buttress Dam,” *Proceedings, 38<sup>th</sup> U.S. Symposium on Rock Mechanics*, Washington, DC, A.A. Balkema, pp. 951-957, 2001.

Scott, G.A. “Probabilistic Stability Analysis – You Can Do It,” *Proceedings, Association of State Dam Safety Officials Conference*, Austin, Texas, 2007.

US Army Corps of Engineers. Technical Memorandum 3-424. 1956 Oct. Investigation of underseepage and its control: Lower Mississippi River levees. Volumes 1 and 2. Vicksburg (MS): Waterways Experiment Station. Prepared for the President, Mississippi River Commission, Corps of Engineers. [http://acwc.sdp.sirsi.net/client/en\\_US/search/asset/1040155](http://acwc.sdp.sirsi.net/client/en_US/search/asset/1040155).

US Army Corps of Engineers. Engineer Technical Letter 1110-2-556, “Risk-Based Analysis in Geotechnical Engineering for Support of Planning Studies,” 28 May 1999.

Vick, S.G., *Degrees of Belief, Subjective Probability and Engineering Judgment*, ASCE Press, Reston, VA, 2002.

Watermeyer, C.F., “A Review of the Classical Method of Design of Medium Height Gravity Dams and Aspects of Base Shortening with Uplift,” *Journal of the South African Institution of Civil Engineering*, Vol 48 No 3, pp. 2-11, 2006.

Wolff, T.F., “Evaluating the Reliability of Existing Levees,” research report prepared for the U.S. Army Engineer Waterways Experiment Station, Michigan State University, September 1994.